ISSN 0020-4412, Instruments and Experimental Techniques, 2012, Vol. 55, No. 2, pp. 187–197. © Pleiades Publishing, Ltd., 2012.
Original Russian Text © I.V. Khodyuk, P.A. Rodnyi, P. Dorenbos, 2012, published in Pribory i Tekhnika Eksperimenta, 2012, No. 2, pp. 44–55.

NUCLEAR EXPERIMENTAL TECHNIQUE

Energy Dependence of the Relative Light Output of $YAlO_3$:Ce, Y_2SiO_5:Ce, and YPO_4:Ce Scintillators

I. V. Khodyuk[a], P. A. Rodnyi[a], and P. Dorenbos[b]

[a] *National Research University, St. Petersburg State Polytechnical University, Laboratory of Ionic Crystal Physics, ul. Politekhnicheskaya 29, St. Petersburg, 195251 Russia*

[b] *Delft University of Technology, Faculty of Applied Physics, Luminescence Materials Research Group, Mekelweg, 15, Delft, 2629 JB, The Netherlands*

Received April 7, 2011; in final form, August 11, 2011

Abstract—The nonlinear dependence of the relative light output on the energy deposited in single-crystal scintillation materials $YAlO_3$:Ce (YAP:Ce), Y_2SiO_5:Ce (YSO:Ce), and YPO_4:Ce (YPO:Ce) has been studied. The investigations have been conducted under quasi-monochromatic X-ray excitation in the energy range of 9.5–100 keV. In addition to the standard technique for measuring the nonproportional scintillator response based on the dependence of the full-energy peak position on the energy of incident radiation, a method is proposed for measuring the light output by X-ray fluorescence peaks. Using this method for YAP:Ce, it is possible to investigate the nonlinear dependence of the light output on the photon energy in the energy range of 2–40 keV. Along with this method, the *K*-dip spectroscopy method has been proposed and tested by measuring the dependence of the relative light output on the electron energy in the range of 0.1–80.0 keV. The processes resulting in the loss of the scintillation material efficiency at a high ionization density are considered.

DOI: 10.1134/S0020441212020054

1. INTRODUCTION

Rapid development of electronics poses new goals and objectives behind researchers and developers of scintillation materials [1]. The wide use of scintillator-based ionizing radiation detectors in vitally important fields, such as medicine, safety, and science, makes the requirements specified for new materials by customers more stringent.

The energy resolution is one of the most significant parameters of a scintillator. Energy resolution R is conventionally defined as ratio $\Delta E/E$, where ΔE is the full width at half-maximum of the full-energy peak, and E is the position of this peak on the energy scale, and is expressed in percent [2]. Available scintillation detectors are inferior to semiconductor detectors in the energy resolution. For example, for a single-crystal $LaBr_3$:Ce scintillator, $R = 2.75\%$ at an incident γ-ray energy of 662 keV [3]. This value is much worse than the energy resolution of the semiconductor detectors based on high-purity germanium, which is 2–4 keV or 0.3–0.6% at an energy of 662 keV [4]. Nevertheless, semiconductor detectors cannot be used now in medical tomography and high-energy physics instead of scintillators, which dominate in these fields [5]. Therefore, development of new scintillation materials with improved characteristics is an urgent and important task.

In this study, we measured the energy resolution and relative light output of YAP:Ce, YSO:Ce, and YPO:Ce scintillators in the energy range of 9.5–100.0 keV using synchrotron radiation. Special emphasis was placed on X-ray fluorescence events. Using information obtained from analysis of the energy spectra at different energies of incident radiation, we succeeded in plotting the relative light output curves in the energy ranges of 2–100 keV for YAP:Ce and 10–100 keV for YSO:Ce and YPO:Ce scintillators. The high energy resolution of the experimental setup has allowed us to take measurements of the relative light output in the energy range of the *K*-electron binding energy of yttrium $E_{KY} = 17.038$ keV with a step of 0.1 keV. Analyzing the results of measurements using the *K*-dip spectroscopy method, the dependence of the relative light output on the *K-electron energy* has been determined in the energy ranges of 0.1–80 keV for YAP:Ce, 1–80 keV for YSO:Ce, and 0.5–80 keV for YPO:Ce.

2. RELATIVE LIGHT OUTPUT NONLINEARITY

2.1. Energy Resolution

Energy resolution R of an ionizing radiation detector based on a scintillator coupled to a photodetector—in our case, to a photomultiplier tube (a PMT)—is determined, according to [7, 8], by the three basic parameters: intrinsic resolution of the scintillation crystal R_{sc}, transport resolution R_{tr}, and resolution of the photodetector (the PMT) R_{ph}. Intrinsic resolution of the scintillation crystal R_{sc} depends on two parameters, one of which is the nonlinear dependence of the relative light output on the incident radi-

ation energy, also known as nonproportionality R_{np}, and the other is inhomogeneity of the scintillation crystal R_{ih}. Therefore, the energy resolution of the detector is defined by the formula:

$$\Delta E/E = R = \sqrt{R_{cs}^2 + R_{tr}^2 + R_{ph}^2} = \sqrt{R_{np}^2 + R_{ih}^2 + R_{tr}^2 + R_{ph}^2}. \quad (1)$$

The inhomogeneity of the scintillator may be caused by the irregular distribution of the luminescence centers inside the crystal or by the presence of various defects, which makes the light yield dependent on the interaction point and contributes to the broadening of the full-energy peak. The R_{np} value is determined by the nonlinear dependence of the light yield on the secondary electron energy, which is often called the nonproportionality. Production of secondary electrons (i.e., photoelectrons, Compton electrons, Auger electrons, etc.) during relaxation of the primary γ-ray energy inside the scintillator is a probabilistic process and may occur in different ways for primary γ rays with the same energy. The total number of photons produced inside the scintillator during interaction with a γ-ray photon with a predetermined energy can be determined by adding the products of the absolute light yield into the energy over all values of secondary electrons. The dependence of the absolute light yield on the energy of secondary electrons and the probabilistic character of relaxation of the primary radiation energy result in variability of the total number of photons produced inside the scintillator. This process also leads to broadening of the full-energy peak in the energy spectrum measured by a scintillation detector.

There are many factors determining the efficiency of photon transport and conversion and thereby affecting the energy resolution. Contributions to transport resolution R_{tr} can also be made by the sensitivity of the PMT photocathode at a certain wavelength of the scintillation light, the self-absorption in the bulk of the scintillator, the efficiency of light collection, the quality of the optical contact between the scintillator and the PMT entrance window, the efficiency of photoelectron collection on the first dynode, and others [6, 7].

The contribution of the PMT R_{ph} to the total energy resolution of the scintillation detector depends on the light output according to the formula [6]

$$R_{ph} = 2.35\sqrt{(1 + \nu(M))/N_{pe}^{PMT}}, \quad (2)$$

where $\nu(M)$ is the dispersion of the gain during multiplication of photoelectrons in the PMT, and N_{pe}^{PMT} is the number of photoelectrons that are produced by the interaction of scintillation photons with the PMT photocathode and are incident on the first dynode [8].

The effect exerted by energy resolution of the PMT R_{ph} on the total energy resolution of the detector decreases with an increase in the light yield in the scintillator and a decrease in the dispersion caused by the PMT. Today, the researchers have approached the maximum of the light yield in the majority of the known scintillators [9]. The maximum of the light yield is primarily determined by the emission wavelength and scintillator's width of the forbidden gap E_g [2, 10]:

$$\frac{N_{ph}\langle h\nu\rangle}{E_\gamma} = Y\frac{h\nu_{max}}{E_g}SQ, \quad (3)$$

where $N_{ph}\langle h\nu\rangle$ is the number of scintillation photons with the averaged radiation energy, E_γ is the energy of primary radiation (as a rule, a value of 1 MeV is used), $Y = E_g/E_{eh} = 1/\beta$ is the efficiency of the ionization process (for most scintillators, β is in the range of 1.5–3.5 [10, 11]), $h\nu_{max}$ is the energy of scintillation photons in the maximum of the luminescence peak, S is the efficiency of the energy transfer from the scintillator matrix to the luminescence centers, and Q is the quantum efficiency of the luminescence process.

In view of the aforesaid, the use of nanocrystalline materials seems to be promising [12], since an increase in the oscillator intensity in an emitting center causes the emission intensity of the luminescence centers in nanocrystals to increase and the luminescence decay time to decrease. Therefore, materials containing nanocrystals are very attractive for development of ultrafast scintillators with a high light yield [13].

2.2. Methods for Measuring the Energy Dependence of the Light Output

The nonlinear dependence of the relative light output on the energy of incident radiation—the nonproportionality—is a significant factor determining the energy resolution [6, 10, 14]. This phenomenon is the key obstacle in designing scintillation detectors of ionizing radiation with improved characteristics. By the nonproportionality of the relative light output is meant the nonlinear dependence of the number of light photons produced in the scintillator, on the absorbed radiation energy. Serious attempts have recently been made to reveal the mechanism of the nonproportionality and develop the theoretical model capable of predicting both the nonproportionality scale and the energy resolution of scintillation materials [15–20]. However, most of the models existing today can only describe available experimental data, but are incapable of predicting the behavior of new scintillators.

For comprehensive understanding of the physical processes resulting in a partial loss of the scintillator efficiency and, hence, in the nonproportionality of the relative light output, we must have an adequate amount of experimental data. Today, there are two main approaches to measuring the nonproportionality. The first of these, which is simpler and better reflects the quality of the material under investigation, is based on measuring the light output of the scintillator as a function of the radiation energy. This method

Table 1. Characteristics of the scintillation materials

Scintillator	Dimensions, mm	Light output at 662 keV, photoelectrons/MeV	Energy resolution at 662 keV, %	Decay time of the scintillation pulse, ns
$YAlO_3$:Ce (YAP:Ce)	∅10 × 0.8	8116 ± 35	5.0	27 [25]
Y_2SiO_5:Ce (YSO:Ce)	8 × 8 × 0.5	2070 ± 24	8.3	42 [26]
YPO_4:Ce (YPO:Ce)	8 × 2 × 0.5	2117 ± 22	31.4	30 [27]

implies the use of radioactive sources, e.g., ^{137}Cs, ^{241}Am, ^{22}Na, ^{55}Fe, etc.

The main drawbacks of this method are the limited number of available radioactive sources and the signal overlapping if a source emits several quanta with close energy values. The substantial limitation may also be imposed by the small absorption length of quanta in the range of low energies (<10 keV) and, therefore, the susceptibility of a result to the absorption in the surface layers of the scintillator. Although the effect exerted both by the surface itself and by the surface layers on the characteristics of inorganic scintillation materials has not yet been systematically investigated, nevertheless, observations of this kind have been mentioned in the literature [15, 21]. Since it is in this energy range that the largest deviations of the relative light output from the linear law are observed, obtaining experimental data in the range of low energies and developing new methods for measuring the nonproportionality are very urgent tasks.

An alternative method for measuring the nonproportionality is the Compton coincidence technique, which was proposed for this purpose by B.D. Rooney and J.D. Valentine in the early 1990s [22] and enhanced by W.S. Choong et al., in 2008 [23]. This technique is based on detecting events of Compton scattering of incident radiation from electrons of the scintillator material. After Compton scattering, a γ-ray photon escapes from the scintillator and is detected by a high-purity germanium detector. The energy resolution of the high-purity germanium detector, which is ~3 keV [4], allows the energy of the scattered γ-ray photon to be estimated with a high degree of accuracy. Knowing the initial and final energies of the γ-ray photon, one can evaluate the energy transferred to a recoil electron inside the scintillator. Simultaneously measuring the light output of the scintillator in the coincidence mode using the PMT, one can establish the unambiguous dependence of the recoil electron energy and the number of light photons produced thereby. Therefore, one can determine the dependence of the relative light output on the electron energy. This method is applicable in a wide energy range, 3–466 keV [24]. Nevertheless, the Compton coincidence technique cannot be used below 3 keV, since the PMT noise starts predominating over the signal arriving from the scintillator.

3. EXPERIMENT

3.1. Scintillation Crystals

Scintillation crystals with various sizes and characteristics were used in the experiment. Some characteristics of the investigated crystals are presented in Table 1. The YAP:Ce sample was a 10-mm-diameter 0.8-mm-thick disk polished on one side. The YSO:Ce crystal was shaped as a parallelepiped polished on all sides, with dimensions of 8 × 8 mm and a thickness of 0.5 mm. The YPO:Ce crystal had the smallest size among the samples under investigation; it was an untreated crystal chip over the cleavage plane ~8 mm long, 2 mm wide, and ≤0.5 mm thick.

The decision to use these crystals in our study was based on the fact that they comprised the same yttrium cation (Y^{3+}) and different anion groups (AlO_3^{3-}, SiO_5^{6-}, and PO_4^{3-}). A change of the anion is followed by a substantial change in the nonproportionality of the relative light output and, hence, in the energy resolution. Though the luminescence mechanisms in these samples are similar, the nonproportionality changes due to relaxation of the Ce^{3+} dopant introduced into all three samples. It can also be noted that a change of the cation is followed by a significant change in the absolute light output (Table 1).

3.2. Absolute Light Output

The absolute light output of the scintillation crystals under investigation was measured using the ^{137}Cs γ-ray source (662 keV). A Hamamatsu R6231-100 PMT was the photodetector. The Ortec 672 preamplifier and spectrometric amplifier were used to amplify and shape the signal arriving at the Ortec 114 16k ADC analog-to-digital converter. The absolute light output was determined by comparing the position of the full-energy peak maximum in the ^{137}Cs spectrum (662 keV) to the position of the center-of-gravity of the single-photoelectron spectrum [28]. To increase the collection efficiency for light photons produced by absorption of γ rays, the samples under investigation were coated with several layers of a reflecting Teflon tape [7]. Optical contact between the scintillation crystal and the PMT photocathode was maintained by a Viscasil 600000 cSt optical lubricant (General Electrics). The shaping time of the Ortec 672 spectrometric amplifier was selected to be the longest possible

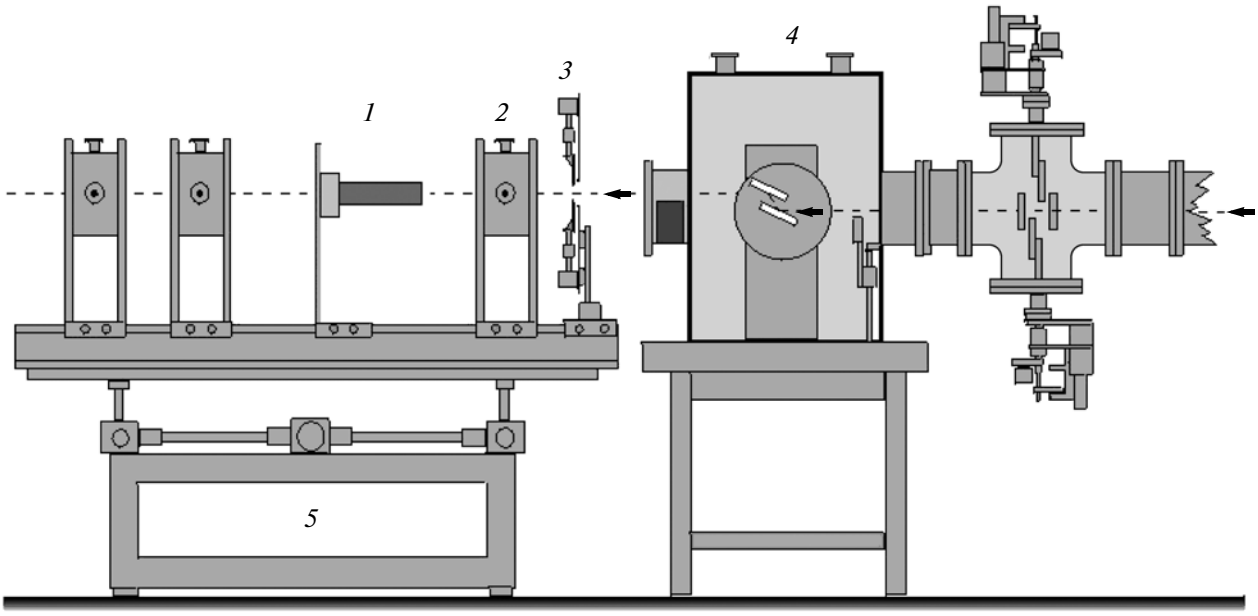

Fig. 1. Diagram of the X-1 experimental station at the Hamburger Synhrotronstrahlungslabor (HASYLAB) synchrotron in Hamburg, Germany: (*1*) detector (scintillator, PMT, and preamplifier), (*2*) ionization chamber, (*3*) exit slit, (*4*) monochromator, and (*5*) adjustable experimental table.

(10 μs), so as to ensure collection of light from long luminescence components.

3.3. Relative Light Output

The relative light output was measured according to the scheme similar to the above-described scheme for the absolute light output. It is nevertheless important that quasi-monochromatic synchrotron radiation was used instead of the ^{137}Cs radioactive source. The experiment was performed at the X-1 experimental station of the HASYLAB synchrotron research complex (Hamburg, Germany). The diagram of the experimental setup is presented in Fig. 1.

A monochromatic X-ray beam was used to excite the scintillation crystals and measure the energy spectra in the energy range of 9.5–100 keV. Owing to the effect of double Bragg reflection of X rays from the quartz crystals of monochromator *4*, the energy resolution values of 1 and 20 eV or better has been obtained at a beam energies of 9.5 and 100 keV, respectively. The geometrical dimensions of the beam were determined by the width of the output slit aperture; in the course of the experiment, they were 50 μm along the horizontal and vertical axes. The PMT with the scintillator attached to its entrance window, the preamplifier, and the auxiliary electronics were fixed in place on the table adjustable along the *X* and *Y* axes with an accuracy of 1 μm and better. Prior to taking each measurement, the position of the table was optimized, so that the counting rate of the detector was the highest. To rule out overlapping of the scintillation pulses and distortion of the output signal, the synchrotron radiation intensity was reduced to values corresponding to the counting rate of a scintillation counter, i.e., ~1 kHz. The detector was shielded on all sides with a 2-mm-thick lead layer, except for the frontal plane of the detector, in order to minimize the noise due to the background radiation at the experimental station. Additional corrections were introduced to the result of measurements in view of the corrections caused by the ADC nonlinearity, and the value of these corrections was determined using an Ortec 419 precision pulse generator with a variable amplitude. All measurements were performed at room temperature.

4. EXPERIMENTAL RESULTS

4.1. Energy Spectra

Figure 2 presents the energy spectra measured for the YAP:Ce scintillation crystal using quasi-monochromatic synchrotron radiation with energies of 15, 20, 50, and 80 keV. Similar spectra were obtained for all the single crystals under investigation in the energy range of 9.5–100 keV. The typical step was 5 keV over the whole energy range. To obtain a more detailed pattern, additional measurements were taken in the region of low X-ray energies (9.5–15 keV) with a step of 1 keV. More rapt attention was focused on the range near the *K*-electron binding energy of an yttrium atom ($E_{KY} = 17.038$ keV). In this region, the measurements were taken with a step of 0.1 keV. From these data, the absolute light output of the scintillator was determined at a selected X-ray energy. By comparing the obtained value to the absolute light output at 662 keV, the rela-

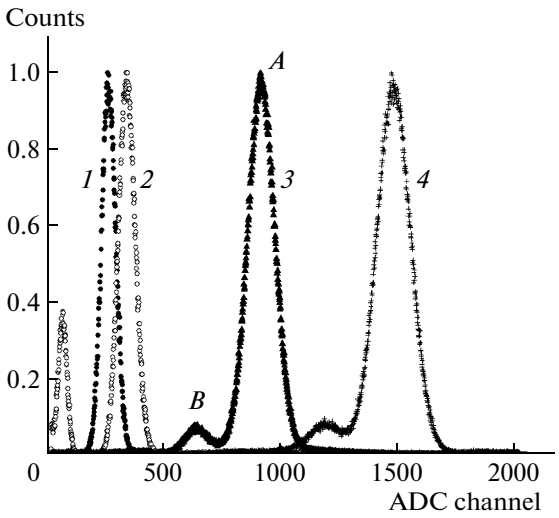

Fig. 2. Measured YAP:Ce energy spectra for monochromatic X rays with energies (*1*) of 15, (*2*) 20, (*3*) 50, and (*4*) 80 keV; (*A*) X-ray full-energy peak; and (*B*) fluorescence peak at an excitation energy of 50 keV.

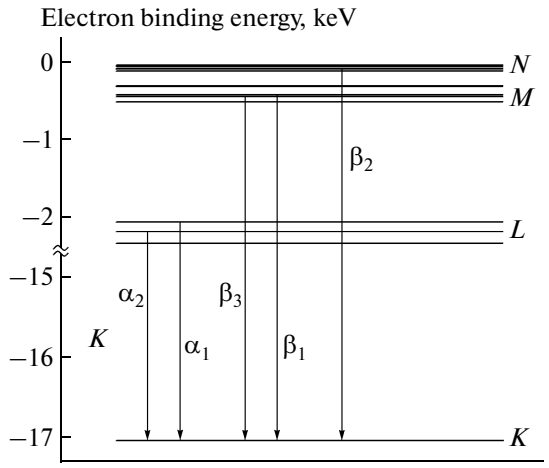

Fig. 3. Most probable transitions in the electron shell of an yttrium atom. X-ray fluorescence.

tive light output was determined for the selected energy.

If the energy of incident synchrotron radiation is higher than the electron binding energy on the *K* shell of an yttrium atom ($E_{KY} = 17.038$ keV), X-ray fluorescence peak (*B*), in addition to a full-energy peak (*A*), is present in the spectra similar to those in Fig. 2. The presence of this peak can be attributed to relaxation of the high-energy excitations in the atom. By contrast to the full-energy peak that has the Gaussian shape, a typical X-ray fluorescence peak is a superposition of a few Gaussian curves. Figure 3 and Table 2 demonstrate the most probable transitions that follow photoabsorption of X rays on the *K* shell of yttrium and result in the formation of X-ray fluorescence peaks [29].

The mechanism of X-ray fluorescence peak formation in energy spectra (peak *B* in Fig. 2) is as follows. An X- or γ-ray photon with energy in the range of 17–100 keV interacts with the substance purely by the mechanism of photoeffect. The higher the binding energy of an electron, the higher the probability of photoeffect; therefore, there is a high probability that, in all three scintillators—YAP:Ce, YSO:Ce, and YPO:Ce—this interaction occurs on a *K* electron of the yttrium atom. The photoeffect results in production of a photoelectron with energy

$$E_e = E_{\text{X-ray}} - E_{KY}, \quad (4)$$

where $E_{\text{X-ray}}$ is the energy of the incident X-ray photon, and $E_{KY} = 17.038$ keV. Production of a photoelectron is followed by formation of a hole on the *K* shell of the yttrium atom. The atom, as it tends to return to the initial nonexcited state, relaxes with the transition of one of the outer electrons to the inner *K* shell (Fig. 3). This transition results in emission of an X-ray fluorescence photon or an Auger electron. The energy of this X-ray fluorescence photon is equal to the difference in the binding energy of an electron on the respective atomic shells (these values are presented in Table 2). If the X-ray fluorescence photon escapes from the scintillator volume without interaction, we can observe a peak similar to the peak in Fig. 2 (*B*). The range of possible Auger electrons, as well as the range of a photoelectron, is extremely short (a few micrometers), and the probability that any of these electrons will escape from the scintillator, carrying away a portion of the energy, is very small and is therefore ignored in our study.

Energy E_{dep} deposited inside the scintillator and associated with the X-ray luminescence peak can be determined from the expression

$$E_{\text{dep}} = E_{\text{X-ray}} - E_{\text{esc}}, \quad (5)$$

where E_{esc} is the energy carried away by the X-ray fluorescence photon, and $E_{\text{X-ray}}$ is the energy of the incident X-ray photon. While fitting the experimental spectra, we proceeded from the five most probable transitions in the atomic shell of yttrium: $K_{\alpha 1}$, $K_{\alpha 2}$, $K_{\beta 1}$, $K_{\beta 2}$, and $K_{\beta 3}$.

The energies and probabilities of these transitions used in determining the absolute and relative light outputs are presented in Table 2. Assuming that each pos-

Table 2. Main *K* transitions at X-ray fluorescence in the electron shell of an yttrium atom [29]

Line	Transition	Energy, keV	Probability
$K_{\alpha 1}$	$K–L_3$	14.958	0.5561
$K_{\alpha 2}$	$K–L_2$	14.882	0.2897
$K_{\alpha 3}$	$K–L_1$	14.665	0.0004
$K_{\beta 1}$	$K–M_3$	16.739	0.0884
$K_{\beta 2}$	$K–N_{2,3}$	17.014	0.0186
$K_{\beta 3}$	$K–M_2$	16.727	0.0458

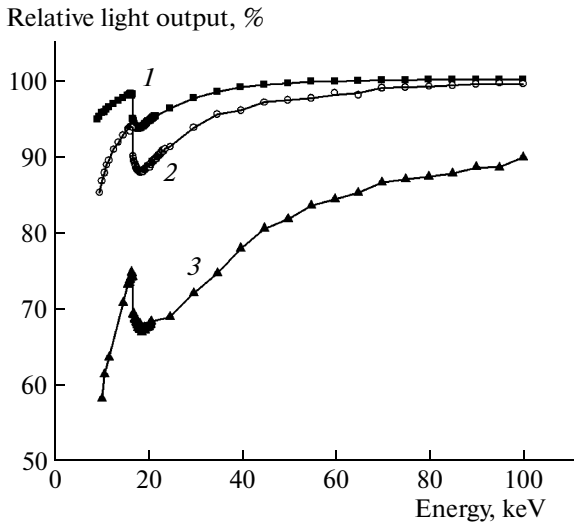

Fig. 4. Relative light output (*1*) of the YAP:Ce, (*2*) YSO:Ce, and (*3*) YPO:Ce scintillators vs. the incident radiation energy. All curves are normalized to 662 keV.

sible transition results in the formation of a separate peak with the Gaussian shape, we used the sum of five Gaussian distributions with equal widths [30] to fit the experimental curves. Since the energy resolution of all the scintillation materials used in this study was inadequate for unfolding the K_α and K_β peaks (Fig. 2), as had been done for the other scintillators in [17, 31], the energy carried away by the X-ray fluorescence photon E_{esc} was assumed to be the weighted average energy of all five transitions. Applying Eq. (5) to all spectra for incident synchrotron radiation energies above $E_{KY} = 17.038$ keV, we obtained the values of the absolute and relative light outputs as functions of the deposited energy.

4.2. Relative Light Output

The relative light output *RLO* at radiation energy *E* is defined as the ratio of absolute light output *ALO* at a fixed energy of incident radiation to the value of this energy *E* expressed in percent of the absolute light output at an energy of 662 keV, divided by 662 keV:

$$RLO(E) = \frac{ALO(E)/E}{ALO(E_0)/E_0}, \qquad (6)$$

where $E_0 = 662$ keV.

The dependences of the relative light output of the YAP:Ce, YSO:Ce, and YPO:Ce scintillators on the energy of incident X rays are presented in Fig. 4. The measurement error, which is not shown in Fig. 4, is 0.5% over the whole energy range.

For all three scintillators under investigation, the behavior of the relative light output is almost the same. In the region of energies higher than 19 keV, a slow decline of the relative light output at energies of <100 keV and a local minimum at 19 keV are observed for all the spectra in Fig. 4. Though the behavior of the curves is approximately the same, nevertheless, the numerical values of the relative light output in different scintillators differ substantially. Thus, for the YAP:Ce scintillator, which exhibits the best proportionality (curve *1* in Fig. 4), the relative light output decreases only slightly (by ~6.4%), from ~100% at an incident radiation energy of 100 keV to 93.6% at 18.3 keV. For the YSO:Ce scintillator (curve *2*), a more substantial decrease in the relative light output is observed in this energy range: it changes from ~100% at 100 keV to 87.9% at 18.7 keV, i.e., by 12.1%. The largest decrease in the relative light output is observed for YPO:Ce (curve *3*): from 89.8% at 100 keV to 67.0% at 18.9 keV, i.e., by 22.8%.

When the synchrotron radiation energy decreases below 19 keV, the behavior of the relative light output is also similar for all these scintillators: after a local minimum at energies of 18.3–18.9 keV, it increases sharply and exhibits a local maximum at energies below the *K*-electron binding energy of an yttrium atom $E_{KY} = 17.038$ keV. The value of the stepwise change in the relative light output depends on the scintillator material, being 4.5, 6.0, and 7.9% for YAP:Ce, YSO:Ce, and YPO:Ce scintillators, respectively. We see that, the smaller the drop of the relative light output in the energy range of 19–100 keV, the smaller the jump at energies of 17–19 keV.

At radiation energies below 17 keV, a similar dynamics of the further decrease in the relative light output is also observed for the YAP:Ce, YSO:Ce, and YPO:Ce crystals. Thus, for YAP:Ce, as the energy decreases from 17.0 to 9.5 keV, the relative light output declined to a value of 94.8%, i.e., by 3.3%. For YSO:Ce, a decrease in the relative light output by 8.6% to a value of 85.3% is observed in the energy range from 17 to 10 keV. The relative light output in YPO:Ce is 58.3% at an incident radiation energy of 10.5 keV, which corresponds to a decrease of 16.6% in the relative light output in the energy range from 17.0 to 10.5 keV.

To make sure that the observed behavior of the relative light output versus the synchrotron radiation energy is correct, additional measurements of this dependence were taken for the YAP:Ce scintillator in the energy range of 16–20 keV at three different points of the crystal separated by 1 mm. Since the geometrical dimensions of the X-ray beam are 50 × 50 μm, these points are considered to be independent. The results of these measurements are shown in Fig. 5. From the figure, it is apparent that both the qualitative behavior and the numerical values of the relative light output in different regions of the YAP:Ce scintillation crystal differ only slightly. The deviations obtained do not exceed the above-mentioned measurement error of 0.5% and are not systematical in character. This is evidence that the shape of the curve of the relative light output does not depend on the local properties of the scintillation material.

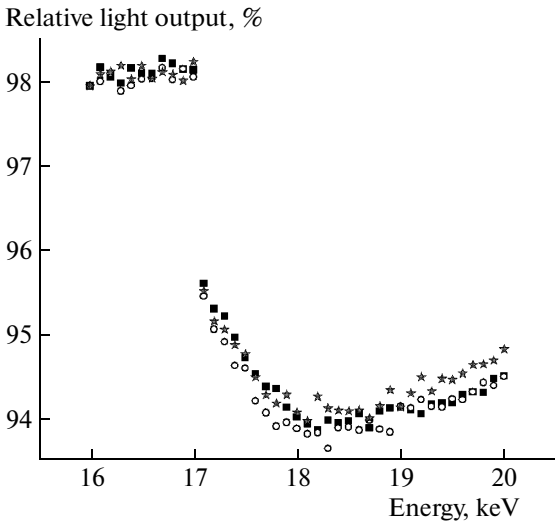

Fig. 5. Variations of the dependence of the YAP:Ce relative light output on the incident radiation energy in the range of *K*-electron binding energy of yttrium at three points on the crystal, spaced apart by 1 mm.

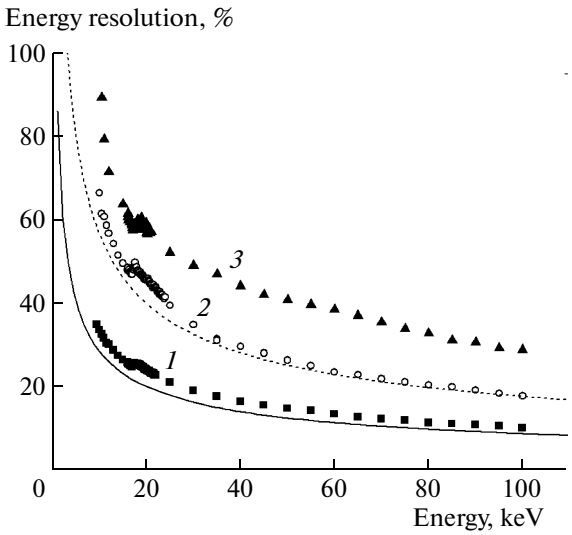

Fig. 6. Energy resolution (*1*) of the YAP:Ce, (*2*) YSO:Ce, and (*3*) YPO:Ce scintillators vs. the incident radiation energy. The PMT resolution obtained according to Eq. (2) is shown with a solid line for YAP:Ce and dashed lines for the YSO:Ce and YPO:Ce scintillators.

4.3. Energy Resolution

The energy resolution is defined as the ratio of the full width at half-maximum ΔE of the full-energy peak (peak *A* in Fig. 2) to the position of this peak on the energy scale E, and ratio $\Delta E/E$ is expressed in percent. The dependences of the energy resolution of the YAP:Ce, YSO:Ce, and YPO:Ce scintillators on the energy of incident synchrotron radiation are presented in Fig. 6. It should be noted that, for the YAP:Ce and YSO:Ce scintillation crystals, these dependences are represented by Eq. (2). In this case, we may conclude that the contributions of such factors as the sample inhomogeneity, the quality of light collection, and the nonproportionality are small relative to the photodetector resolution. However, this conclusion cannot be applied to the energy dependence of the YPO:Ce resolution, which demonstrates a significant departure from the theoretical curve in Fig. 6.

The energy resolution of the YAP:Ce and YSO:Ce scintillators decreases in the energy range of 9.5–100 keV from 34.9 to 10.4% and from 66.3 to 18.0%, respectively. In addition, there is a small jump in the region corresponding to the *K*-electron binding energy of yttrium $E_{KY} = 17.038$ keV: ~1.0 and 2.8%, respectively. These data are in good agreement with the results obtained using the other methods in [32, 33]. The worst energy resolution is exhibited by the YPO:Ce scintillator: 89.1% for an excitation energy of 10.5 keV and 29.0% for 100 keV. The significant discrepancy between the measured behavior of the energy resolution and the theoretical curve (see Fig. 6) and its large values are likely to be caused by the inhomogeneity of the scintillator sample. Potentially, the energy resolution of the YPO:Ce scintillator may be improved by improving the optical properties of the scintillation crystal.

4.4. X-ray Fluorescence

To obtain additional information on the relative light output in the region of low energies, we analyzed the X-ray fluorescence peaks (*B* in Fig. 2). Using the algorithm described in Subsection 4.1, we plotted the dependence of the relative light output on the energy deposited inside the YAP:Ce scintillator. The results obtained by analyzing the positions of X-ray fluorescence peaks versus the energy of incident synchrotron radiation are presented in Fig. 7. We failed to plot similar curves for the YSO:Ce and YPO:Ce scintillators, since they exhibited a low light output and a poor energy resolution in the energy range under investigation (Table 1, Fig. 6).

The results of the analysis of the full-energy peaks (curve *1*) and the X-ray fluorescence peaks (curve *2*) are shown in Fig. 7. One can see the discrepancy between the values of the relative light output in the region of energies where the results were obtained using two methods. For example, at a deposited energy of 9.9 keV, the relative light output obtained using the X-ray fluorescence peaks is 92.3%, whereas the value obtained at synchrotron radiation energy of 10 keV is 95.2%. The difference of 2.9% cannot be explained by the error of measurements, since it is only 0.5% at these energies for both of the methods. Therefore, we have systematic differences that lead to this result. A similar pattern is observed at higher deposited energies. It should nevertheless be noted that, as the energy grows in value, the difference in the relative light output decreases, reaching 1% at 35 keV.

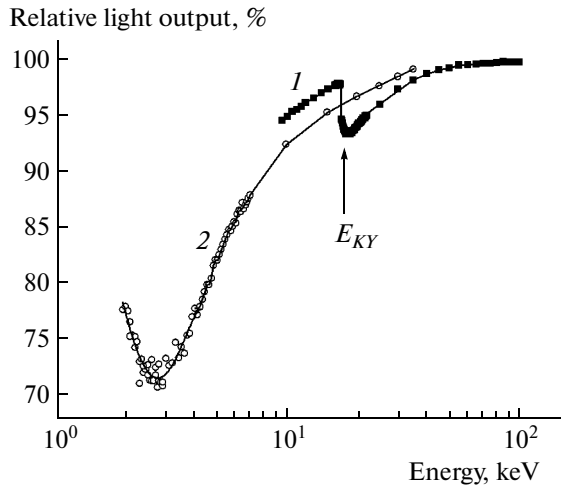

Fig. 7. Dependences of the relative light output on the energy deposited in the YAP:Ce scintillator, obtained by analyzing (*1*) the full-energy peaks and (*2*) the X-ray fluorescence peaks.

Let us try to describe the observed discrepancy in the relative light output by analyzing the mechanism of interaction and relaxation of high-energy excitation in the scintillation material. Compare the most probable ways in which the full-energy and X-ray fluorescence peaks are formed. The mechanism of X-ray fluorescence peak formation has already been described in Subsection 4.1. Let us remind the key statements: the interaction proceeds by photoeffect, a photoelectron and a hole are produced on the *K* shell of an yttrium atom, the hole relaxes to emit an X-ray fluorescence photon, and this photon escapes from the scintillator volume without interaction, carrying away a portion of the energy.

Let us now consider the possible mechanisms of interaction in the case of a full-energy peak. It should be noted that there are many variants of such interactions, and, in this paper, we consider only the main mechanisms.

We assume that the incident radiation energy does not exceed the *K*-electron binding energy of yttrium $E_{KY} = 17.038$ keV. In this case, the interaction with one of the *L* electrons of an yttrium atom or, for the YAP:Ce scintillator, with the *K*electron of an aluminum atom ($E_{K\mathrm{Al}} = 1.559$ keV) becomes most probable. It should be noted that the probability of interaction with the *L* electron of an yttrium atom is practically equal for all three orbitals in this atom; whereas, in the case of X-ray fluorescence, the probability of an electron transition from the L_1 to the *K* shell is substantially smaller than for the L_2 and L_3 (see Table 2). Therefore, we can assume that the difference in the relative light output values obtained using the X-ray fluorescence peaks and the full-energy peaks is caused by the difference in the course of secondary relaxation of electron excitations.

Let us now consider the situation when the energy of incident radiation exceeds the E_{KY} value. The energy relaxation process is similar both for the X-ray fluorescence peaks and for the full-energy peaks. In this case, a significant difference is observed for the energies of a photoelectron produced during photoabsorption on the *K* shell of yttrium. In full-energy peak formation, the value of this energy is described by Eq. (4) and is equal to the difference between the synchrotron radiation energy and the electron binding energy. However, when the X-ray fluorescence peak is formed, a portion of the energy is carried away from the scintillator volume. Therefore, if we consider the situation when the deposited energies for the full-energy and X-ray fluorescence peaks are equal (Fig. 7), the energy carried away from the scintillator must be compensated for by the higher photoelectron energy. For example, at a deposited energy of 35 keV, the photoelectron energy for the case of the full-energy peak is

$$E_e = E_{\text{X-ray}} - E_{KY} = 35\ \text{keV} - 17\ \text{keV} = 18\ \text{keV},$$

whereas, for the X-ray fluorescence peak,

$$E_e = E_{\text{X-ray}} - E_{KY} + E_{\text{esc}} = 35\ \text{keV} - 17\ \text{keV} + 15\ \text{keV} = 33\ \text{keV}.$$

It is this difference in the photoelectron energy that is responsible for the difference in the relative light outputs for different peaks in a spectrum.

The dependence of the relative light output on the energy of incident X or γ rays is the direct consequence of its more fundamental dependence on the secondary electron energy [34]. As the X-ray energy approaches the *K*-electron binding energy in the shell of an yttrium atom, the energy spectrum of secondary electrons is shifted toward lower energies. This shift causes the ionization density to increase, which in turn leads to a decrease in the efficiency of the scintillation material and, as a consequence, to the deterioration of the absolute and relative light outputs [35]. To analyze these processes, we must know the dependence of the relative light output on the electron energy. With this aim in mind, we developed the *K*-dip spectroscopy method, which is described in the next subsection.

4.5. K-dip Spectroscopy

Using the *K*-dip spectroscopy method [34], we plotted the dependence of the relative light output on the *K*-electron energy in the following ranges: 0.1–80 keV for YAP:Ce, 1–80 keV for YSO:Ce, and 0.5–80 keV for YPO:Ce scintillators (Fig. 8). The idea behind the method can be briefly described as follows. Let us assume that an X-ray photon interacts via photoeffect with the *K* electron of an yttrium atom, which results in production of a photoelectron with the energy that can be calculated by Eq. (3), and a hole in the yttrium *K* shell. Thereafter, the hole relaxes in one or another way with the emission of a cascade of secondary X-ray fluorescence photons and Auger elec-

trons. Based on these premises, we can divide the total light output in the scintillator into two components: the light output due to relaxation of the hole on the K shell of yttrium (the K cascade) and the light output due to the photoelectron interaction. Assuming that these components are independent and that the light output due to the K cascade is independent of the initial excitation energy, we can infer that an increase in the incident synchrotron radiation energy is followed by an increase in the photoelectron energy. Therefore, assuming that the light output resulting from the K cascade is equal to the light output at incident radiation energy $E_{\text{X-ray}} = 17.038$ keV [34] and subtracting it from the total light output, we obtain the light output due to the photoelectron. Knowing the photoelectron energy, which is defined as the difference of the incident radiation energy and the K-electron binding energy in the yttrium atomic shell $E_{KY} = 17.038$ keV, and knowing the light output, we obtain the dependence of the relative light output on the K-electron energy. Figure 8 presents the relative light output as a percentage of its value at excitation by γ rays with an energy of 662 keV.

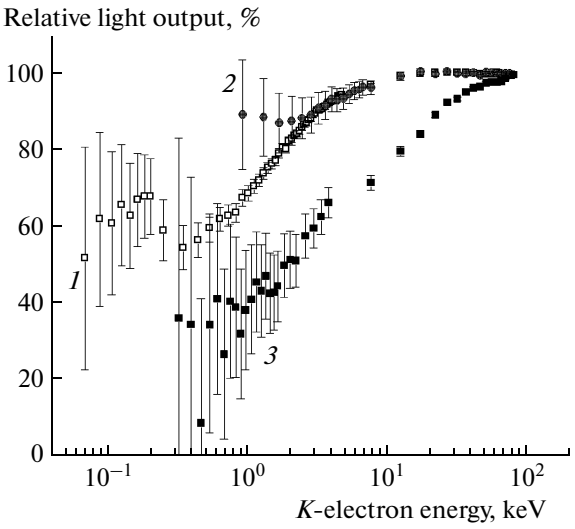

Fig. 8. Relative light output (*1*) of the YAP:Ce, (*2*) YSO:Ce, and (*3*) YPO:Ce scintillators vs. the K-electron energy. The curves were obtained using the K-dip spectroscopy method.

Of the scintillator samples under investigation, the YSO:Ce crystal demonstrates the best proportionality of its dependence of the relative light output on the K-electron energy (curve *2* in Fig. 8). It should nevertheless be noted that the error of this method is large, and the discrepancy in the relative light output of the YAP:Ce and YSO:Ce crystals is fully covered by the measurement error in the energy range of 1–4 keV. The YPO:Ce crystal exhibits a significantly worse proportionality (curve *3* in Fig. 8). The relative light output of this scintillator is ~100% at an electron energy of 80 keV and falls to 30% at an energy of 0.5 keV. Unfortunately, we have no information on other measurements of the nonproportionality in the light output of the YPO:Ce crystal and, hence, cannot compare it to any other results. The only scintillation material, for which we have succeeded in finding data on the dependence of the relative light output on the electron energy, is YAP:Ce. Analyzing the data in [35] and comparing them to the results of our measurements, we note that purely proportional behavior is characteristic of the YAP:Ce scintillator in the energy range of >10 keV. However, as is seen in Fig. 8 (curve *1*), the behavior of the relative light output curve for YAP:Ce does not differ from the behavior of similar curves for other scintillators [17, 31], except for the fact that the light output starts declining at lower electron energies.

5. DISCUSSIONS AND CONCLUSIONS

The nonproportionality of scintillators is considered to be caused by nonradiative recombination of electron–hole pairs (quenching), which exhibits a nonlinear dependence on the ionization density [16, 18, 36–38]. Together with the variability of the local ionization density along an electron track, this process causes the energy resolution of scintillation materials to deteriorate. Proceeding from the above premises, we draw the conclusion that the mobility of the charge carriers (electrons and holes) exerts a significant effect on the nonproportionality [36]. Table 3 presents the values of the nonproportionality of the scintillators in the energy range of 1–80 keV and the effective masses of the carriers [39].

A cloud of electron–hole pairs produced by interaction of a high-energy electron with the scintillator material possesses a very high gradient of the radial carrier concentration along the track. Since the nonlinear recombination processes dependent on the radial component to the fourth or sixth power are considered to be the main sources of nonproportionality in inorganic scintillators [16, 40], the radial diffusion of charge carriers over ~10 ps may be the substantial factor affecting the processes in the scintillators [36]. Based on the numerical models of the transfer and nonlinear quenching, the mechanisms affecting the local light output depending on the excitation density, mobility of the charge carriers, and the exciton diffusivity for a CsI:Tl scintillator were revealed in [38].

The main point of the model presented in [38] is as follows. The finite element method is used to solve the diffusion equation and determine the diffusion currents, the electric fields, and the local carrier densities in a cylindrical volume of space with a radius of 3 nm around the primary electron track. A change in the track radius from 3 to 5 nm does not lead to an appreciable effect [39]. The longitudinal diffusion component is ignored, since the typical length of an electron track exceeds the perpendicular component by ~4–5 orders of magnitude [19]. Therefore, the sought equa-

Table 3. Properties of the scintillation crystals [39]

Scintillator	Nonproportionality [%] relative to 662 keV		Effective mass of the charge carriers (m_0)	
	1 keV	80 keV	electrons	holes
YAP:Ce	~70	100	2.335	1.941
YSO:Ce	~90	100	0.699	3.795
YPO:Ce	~40	100	–	–

tions can be solved in the cylindrical coordinate system as a function of the radius. To take into account the longitudinal dependence of the ionization density, different values of the carrier density were used (in proportion to dE/dx) [16].

Using the values of the effective masses presented in Table 3 and the bimolecular quenching coefficient measured in [18, 41], we obtain a good agreement between the calculation and the experimental values of the light output at electron energies of ~0.1 to 100 keV (Fig. 9). As a result, we say that the nonproportionality of the scintillators is caused by the nonradiative recombination of electron–hole pairs. From the coincidence of the experimental results and the curve obtained by the simulation (see Fig. 9), we draw a conclusion that the mobility of charge carriers has a substantial influence on the nonproportionality effect. Nevertheless, we note that the experimental data available today do not allow unambiguous interpretation of the results. Further investigations must be performed to ascertain the true nature of the nonproportionality phenomenon in inorganic scintillation materials and develop methods capable of minimizing it.

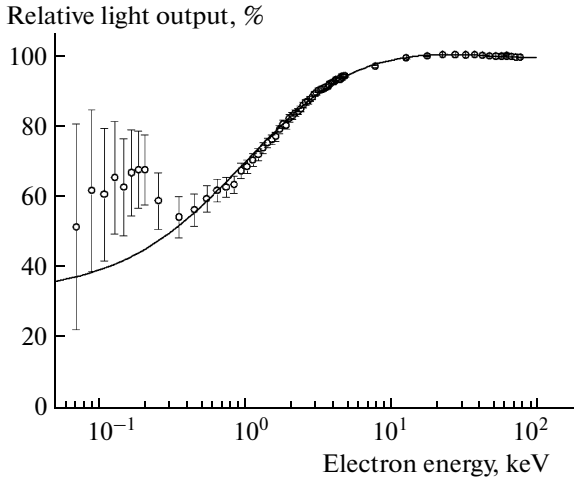

Fig. 9. Comparison of the experimental (dots) and calculated (a curve) relative light output of the YAP:Ce scintillator.

6. CONCLUSIONS

The nonproportionality of the relative light output in YAP:Ce, YSO:Ce, and YPO:Ce scintillation materials versus the energy deposited in them has been investigated under quasi-monochromatic X-ray excitation in the energy range of 9.5–100 keV. In addition to the standard technique for measuring the nonproportional scintillator response, which is based on determining the dependence of the full-energy peak position on the incident radiation energy, a method has been proposed, which allows the nonproportionality of the light output to be determined from the X-ray fluorescence peaks. The use of this method for the YAP:Ce scintillator has made it possible to investigate the nonproportionality effect as a function of the photon energy in the energy range of 2–40 keV. In addition, we developed a technique, called the *K*-dip spectroscopy, with which we succeeded in obtaining the dependence of the relative light output on the electron energy in the range of 0.1–80 keV. These experimental results were compared to the calculations for the YAP:Ce scintillator, performed on the basis of the finite element method.

Of all the scintillators under investigation, the YAP:Ce scintillator exhibits the best linearity in the dependence of its relative light output on the photon energy. Nevertheless, the behavior of the relative light output in YAP:Ce does not differ from the behavior of similar curves obtained for other inorganic scintillators [42], except for the fact that the relative light output starts declining at lower electron energies. The best proportionality of the YAP:Ce scintillator can be attributed to the fact that, according to [38], holes and electrons produced in the ionization process have close values of their mobility. Therefore, it is the exciton states produced by the charge carriers that should be considered in the diffusion process instead of the charge carriers; this will reduce the probability of their quenching in the region of high ionization density.

The dependence of the relative light output on the energy of incident X and γ rays is the direct consequence of a more fundamental dependence of the energy of secondary electrons. As the X-ray energy approaches the binding energy of a *K* electron in the yttrium atomic shell, the energy spectrum of secondary photoelectrons is shifted toward lower energies. This shift leads to an increase in the ionization density, which in turn lowers the efficiency of the scintillation material and, as a result, causes the absolute and relative light outputs to decrease.

The nonproportionality of scintillators results from nonradiative recombination of electron–hole pairs, which exhibits a nonlinear dependence on the ionization density. This process, together with the variability of the local ionization density along an electron track, causes the energy resolution of scintillation materials to deteriorate. The good agreement between the experimental results and the curve obtained by simula-

tion (see Fig. 9) indicates that the nonproportionality effect is strongly affected by the mobility of the electron and hole charge carriers.

It should be noted that there are a lot of semiconductor materials (e.g., ZnO) with a high mobility of the electron and hole charge carriers [43]. In this connection, the use of semiconductor materials based on ZnO as scintillation materials shows much promise [44]. Owing to the linear energy dependence of the relative light output in ZnO, scintillators based on it will exhibit a high efficiency and a high energy resolution.

REFERENCES

1. Schaart, D.R., Seifert, S., Vinke, R., et al., *Physics in Medicine and Biology*, 2007, vol. 55, pp. N179–N189.
2. Rodnyi, P.A., *Physical Processes in Inorganic Scintillators*, New York: CRC Press, 1997.
3. Swiderski, L., Moszyn'ski, M., Nassalski, A., et al., *IEEE Trans. Nucl. Sci.*, 2009, vol. 56, pp. 2499–2505.
4. Owens, A., *IEEE Trans. Nucl. Sci.*, 2008, vol. 55, p. 1430.
5. Van Eijk, C.W.E., *Nucl. Instrum. Methods Phys. Res., Sect. A: Acceler., Spectr., Detect. Assoc. Equip.*, 2003, vol. 509, pp. 17–25.
6. Dorenbos, P., de Haas, J.T.M., and van Eijk, C.W.E., *IEEE Trans. Nucl. Sci.*, 1995, vol. 42, p. 2190.
7. de Haas, J.T.M. and Dorenbos, P., *IEEE Trans. Nucl. Sci.*, 2008, vol. 55, p. 1086.
8. de Haas, J.T.M., Dorenbos, P., and van Eijk, C.W.E., *Nucl. Instrum. Methods Phys. Res., Sect. A: Acceler., Spectr., Detect. Assoc. Equip.*, 2005, vol. 537, p. 97.
9. Dorenbos, P., *IEEE Trans. Nucl. Sci.*, 2010, vol. 57, p. 1162.
10. Rodnyi, P.A., Dorenbos, P., and van Eijk, C.W.E., *Phys. Status Solidi B*, 1997, vol. 187, p. 15.
11. Rodnyi, P.A., *Rad. Measur.*, 1998, vol. 29, p. 235.
12. Klassen, N.V., Kedrov, V.V., Kurlov, V.N., et al., *IEEE Trans. Nucl. Sci.*, 2008, vol. 55, p. 1536.
13. Grigorjeva, L., Millers, D., Smits, K., et al., *Opt. Mater.*, 2009, vol. 31, p. 1825.
14. Lyapidevskii, V.K. and Ryazanov, M.I., *Tech. Phys.*, 2000, vol. 45, p. 948.
15. Kudin, A.M., Grinyov, B.V., Gres', V.Y., et al., *Funct. Mater.*, 2006, vol. 13, p. 54.
16. Bizarri, G., Moses, W.W., Singh, J., et al., *J. Appl. Phys.*, 2009, vol. 105, p. 044507.
17. Khodyuk, I.V. and Dorenbos, P., *J. Phys.: Condens. Matter*, 2010, vol. 22, p. 485402.
18. Williams, R.T., Grim, J.Q., Li, Q., et al., *Phys. Status Solidi B*, 2011, vol. 248, p. 426.
19. Jaffe, J.E., *Nucl. Instrum. Methods Phys. Res., Sect. A: Acceler., Spectr., Detect. Assoc. Equip.*, 2007, vol. 580, p. 1378.
20. Kerisit, S., Rosso, K.M., Cannon, B.D., et al., *J. Appl. Phys.*, 2009, vol. 105, p. 114915.
21. Meggitt, G.C., *Nucl. Instrum. Methods*, 1970, vol. 83, no. 2, pp. 313–316.
22. Rooney, B.D. and Valentine, J.D., *IEEE Trans. Nucl. Sci.*, 1996, vol. 43, p. 1271.
23. Choong, W.-S., Vetter, K.M., Moses, W.W., et al., *IEEE Trans. Nucl. Sci.*, 2008, vol. 55, p. 1753.
24. Choong, W.-S., Hull, G., Moses, W.W., et al., *IEEE Trans. Nucl. Sci.*, 2008, vol. 55, p. 1073.
25. Baryshevsky, V.G., Korzhik, M.V., Moroz, V.I., et al., *Nucl. Instrum. Methods Phys. Res., Sect. B: Beam Inter. Mater.*, 1991, vol. 58, p. 291.
26. Melcher, C.L., Schweitzer, J.S., Peterson, C.A., et al., *Inorganic Scintillators and Their Applications,* Delft: University Press (SCINT95), 1996, p. 309.
27. Ropp, R.C., *J. Luminescence*, 1970, vol. 3, p. 152.
28. Bertolaccini, M., Cova, S., and Bussolati, C., *Proc. Nucl. Electr. Symp.*, Versailles, France, 1968.
29. Thompson, A.C., *X-ray Data Booklet*, *Berkeley: Lawrence Berkeley National Laboratory*, 2009.
30. Moszynski, M., Balcerzyk, M., Czarnacki, W., et al., *IEEE Trans. Nucl. Sci.,* 2004, vol. 51, p. 1074.
31. Khodyuk, I.V., Rodnyi, P.A., and Dorenbos, P., *J. Appl. Phys.*, 2010, vol. 107, p. 113513.
32. Moszyn'ski, M., Kapusta, M., Wolski, D., et al., *Nucl. Instrum. Methods Phys. Res., Sect. A: Acceler., Spectr., Detect. Assoc. Equip.*, 1998, vol. 404, p. 157.
33. Requicha Ferreira, L.F., Ferreira, H.M.N.B.L., Veloso J.F.C.A., et al., *Nucl. Instrum. Methods Phys. Res. Sect. A: Acceler., Spectr., Detect. Assoc. Equip.*, 2004, vol. 516, p. 486.
34. Khodyuk, I.V., de Haas, J.T.M., and Dorenbos, P., *IEEE Trans. Nucl. Sci.,* 2010, vol. 57, p. 1175.
35. Mengesha, W., Taulbee, T.D.R., Rooney, B.D., et al., *IEEE Trans. Nucl. Sci.*, 1998, vol. 45, p. 456.
36. Li, Q., Grim, J.Q., Williams, R.T., et al., *Nucl. Instrum. Methods Phys. Res., Sect. A: Acceler., Spectr., Detect. Assoc. Equip.*, 2010. doi:10.1016/j.nima.2010.07.074
37. Khodyuk, I.V., Alekhin, M.S., de Haas, J.T.M., et al., *Nucl. Instrum. Methods Phys. Res., Sect. A: Acceler., Spectr., Detect. Assoc. Equip.*, 2011, vol. 642, p. 75.
38. Li, Q., Grim, J.Q., Williams, R.T., et al., *J. Appl. Phys.*, 2011, vol. 109, p. 123716.
39. Setyawan, W., Gaume, R.M., Feigelson, R.S., et al., *IEEE Trans. Nucl. Sci.*, 2009, vol. 56, p. 2989.
40. Vasil'ev, A.N., *IEEE Trans. Nucl. Sci.,* 2008, vol. 55, p. 1054.
41. Williams, R.T., Li, Q., Grim, J.Q., et al., *Proc. SPIE 7805 Conf. on Hard X-Ray, Gamma-Ray, and Neutron Detector Physics XII*, 2010.
42. Khodyuk, I.V., Rodnyi, P.A., Gorokhova, E.I., et al., *Nauch.-Tekhn. Vedomosti SPBGPU*, 2010, no. 109, p. 28.
43. Look, D.C., Reynolds, D.C., Sizelove, J.R., et al., *Solid State Commun.,* 1998, vol. 105, p. 399.
44. Rodnyi, P.A., Khodyuk, I.V., and Gorokhova, E.I., *Tech. Phys. Lett.*, 2010, vol. 36, no. 8, pp. 714–715.